INTERNATIONAL JOURNAL OF AUTOMOTIVE AND MECHANICAL ENGINEERING
ISSN: 2229-8649 e-ISSN: 2180-1606
VOL. 22, ISSUE 1, 2025, 11954 – 11964
DOI: https://doi.org/10.15282/ijame.22.1.2025.2.0919

RESEARCH ARTICLE

Thermal Investigation of Heat Transfer Enhancement in a Rectangular Duct Provided with Different Configurations of Semi-Circular Ribs

Swapnil Thikane[1]*, Suresh Mashyal[2]

[1]Faculty of Mechanical Engineering, Sanjay Ghodawat Institute-416118, Visvesveraya Technological University, Belgavi, India
[2]Faculty of Mechanical Engineering, Maratha Mandals Engineering College-591113, Visvesveraya Technological University, Belgavi, India

ABSTRACT – Past research studies have explored the use of continuous ribs (with square or rectangular cross-sections) to improve the thermal efficiency of ducts or channels. Some researchers have also investigated the impact of different rib shapes, such as triangular, semi-circular, trapezoidal, and pentagonal, on thermal performance. However, there has been limited research focusing on how various semi-circular rib patterns influence the thermal behavior of rectangular ducts. This study investigates the effects of different semi-circular rib designs on the thermal efficiency and friction factor of a rectangular duct. Six distinct rib configurations, ranging from continuous to hybrid patterns, were applied to the bottom wall of the test section. The thermo-hydraulic performance (η) of the ribbed ducts was measured and compared to that of plain ducts. Experimental results revealed that the ratio of Nusselt numbers ranged from 1.44 to 2.57. The ratio of the friction factor ranged from 2.20 to 4.51. The thermal enhancement ratios for semi-circular rib designs ranged from 1.08 to 1.69 relative to a plain duct. The hybrid rib configuration surpassed all other rib designs, delivering the most significant improvement in thermal performance. This was primarily due to enhanced flow distribution and reduced thermal resistance. The superior performance of the hybrid ribs resulted from their innovative design, which combines ribs truncated at both ends with ribs truncated at the center, creating a unique hybrid rib arrangement from the combined rib design. Across the specified range of Reynolds numbers, the hybrid rib duct demonstrated a thermal performance increase of 1.47 to 1.69 times compared to the plain duct.

ARTICLE HISTORY
Received : 14th May 2024
Revised : 20th Nov. 2024
Accepted : 30th Dec. 2024
Published : 20th Feb. 2025

KEYWORDS
Reynolds number
Semi-circular rib
Nusselt number
Thermal performance
Friction factor

1. INTRODUCTION

Modern heat exchangers are designed to boost heat transfer rates by incorporating ribs or obstacles in the flow paths [1]. Numerous studies have examined different types of turbulators to improve the thermal efficiency of ducts and channels. Geometric factors such as rib shape, duct size, rib orientation, and the pitch-to-height ratio of ribs are key in enhancing the thermal performance of rectangular ducts [2,3]. Transversely positioned ribs with taper or chamfer were found to increase the pressure drop and friction factor by three times, with a 15° chamfer angle showing the highest pressure drop [4]. Further studies examined ducts with broken crosswise ribs at Reynolds numbers up to 12,000, observing a 1.4 times increase in the heat transfer coefficient compared to plain ducts [5]. Hybrid ribs combining semi-circular and rectangular shapes outperformed individual rib types, showing better performance at Reynolds numbers up to 86,500 [6]. Additionally, various rib configurations were tested in a rectangular duct with an aspect ratio of 4 and pitch-to-breadth ratios ranging from 5 to 10, with boot-shaped ribs providing superior thermal performance [7].

Vortex generators with sloped ribs in rectangular channels showed optimal heat transfer when the ribs had an attack angle of 45° or 60° [8]. The thermal performance of rectangular ducts with rib-roughened opposite walls was also studied under varying Reynolds numbers, aspect ratios, rib angles, and channel blockage ratios [9]. Performance curves typically showed a peak at either 45° or 60° rib inclination, with a minimum at 50° and a maximum at 60° due to the staggered arrangement of ribs [10]. Research comparing various rib arrangements concluded that V-shaped discrete rib configurations outperformed other designs [11]. V-shaped ribs increased heat transfer by 2.83 times and the friction factor by 2.30 times compared to ducts without artificial roughness [12]. The thermal performance of ducts with V-downstream broken ribs was also improved [13,14]. Prismatic ribs attached to the lower surface of a flow passage provided significantly higher thermal performance than square ribs, with a lower friction penalty [15].

Similarly, pentagonal ribs improved heat transfer with a lower pressure penalty compared to square ribs [16]. Numerical studies on concave and convex curved ribs showed that convex fractured ribs provided the best performance, increasing heat transfer rates [17]. Studies on intersecting ribs in high aspect ratio ducts showed that intersecting ribs enhanced heat transfer [18]. Similarly, numerical analysis of ribbed surfaces showed a 50% improvement in thermal performance for corrugated surfaces with a height-to-width ratio of 0.2 [19]. Experimental research was done to determine how different half-round rib configurations affected the thermal performance and friction in a rectangular duct. Using a Reynolds number range of 13,500 to 34,800, six rib configurations—from continuous to hybrid arrangements—were tested. With friction factor ratios ranging from 1.70 to 4.51 and Nusselt number ratios between 1.36 and 2.74, the hybrid

*CORRESPONDING AUTHOR | Swapnil Thikane | ✉ swapnilthikane4444@gmail.com

rib configuration was found to have the greatest thermal enhancement. With enhancement ratios ranging from 1.45 to 1.80 times that of a plain duct, the hybrid configuration offered the best thermal performance overall [20,21]. Additionally, the main findings of numerous investigations carried out by researchers regarding the effects of various flow blocker configurations on the roughness and thermal properties of air heaters. Analyses similar to this one were conducted using the ANSYS FLUENT V16 software to examine the impact of circular and half-round ribs on the enhancement of air heater thermal performance. According to the results, the Reynolds number value of 15,000 had the highest thermal enhancement factor of 1.76 [22-26].

To investigate the impact of pitch on rib roughness, an experimental analysis of a solar air heater with artificial roughness was conducted. It was determined from the analysis that ribs with pitch= ¼ perform better than those with other rib roughness [27]. Additionally, an experimental investigation was conducted to enhance heat transfer using a solar air heater duct equipped with obstacles of six distinct shapes. The findings demonstrated that, out of all the shapes, the staggered arrangement of isosceles trapezoid obstacles has the best thermal performance [28]. Furthermore, an experimental investigation was conducted to examine the impact of a solar air heater with an absorber plate equipped with a winglet-type vortex generator on the characteristics of the friction factor and Nusselt number. During this study, correlations for the friction factor and Nusselt number were created [29]. The enhancement of heat transfer in a rectangular duct with a single corrugated surface was investigated using a similar type of experimental and numerical analysis. According to the findings, the corrugated surface with ribs and a height-to-width ratio of 0.2 showed a 50% improvement in thermal performance [30]. Furthermore, a numerical study of a solar air heater with artificial roughness was conducted using three sets of height and twelve sets of pitch, respectively. According to the findings, semi-circular ribs with a 20 mm pitch and a 2 mm rib height improved overall thermal performance by 98% when compared to a plain heater [31, 32].

A review of the literature reveals several key findings: most studies have focused on using continuous ribs with square or rectangular cross-sections to enhance the thermal efficiency of ducts or channels. Additionally, some researchers have investigated the impact of staggered arrangements of truncated or broken ribs, often with rectangular or square cross-sections, on the thermal performance of rectangular ducts. A few studies have also explored the effects of ribs with various shapes, such as triangular, semi-circular, trapezoidal, and pentagonal. However, there has been limited research on how different semi-circular cross-sectional rib patterns influence the thermal performance of rectangular ducts, presenting an opportunity for further investigation into the use of various semi-circular rib designs within ducts to improve thermal efficiency.

2. EXPERIMENTAL SET-UP AND TEST PROCEDURE

An experimental set-up was constructed to investigate heat transmission and friction qualities inside an open-loop system. The arrangement includes a rectangular duct with several semi-circular rib configurations. There are three sections to the rectangular duct: entrance, test, and exit. Figure 1 illustrates a schematic diagram, while Figure 2 represents a photograph showing the setup of the experiment. Referring to Figure 1, the test configuration consists of (1) a blower with a flow control valve, (2) an entrance section, (3) a test section, (4) an exit section, (5) an anemometer, (6) a digital micromanometer, (7) a test plate with ribs and heater, and (8) a control panel for managing and monitoring airflow, pressure, and temperature conditions during experiments.

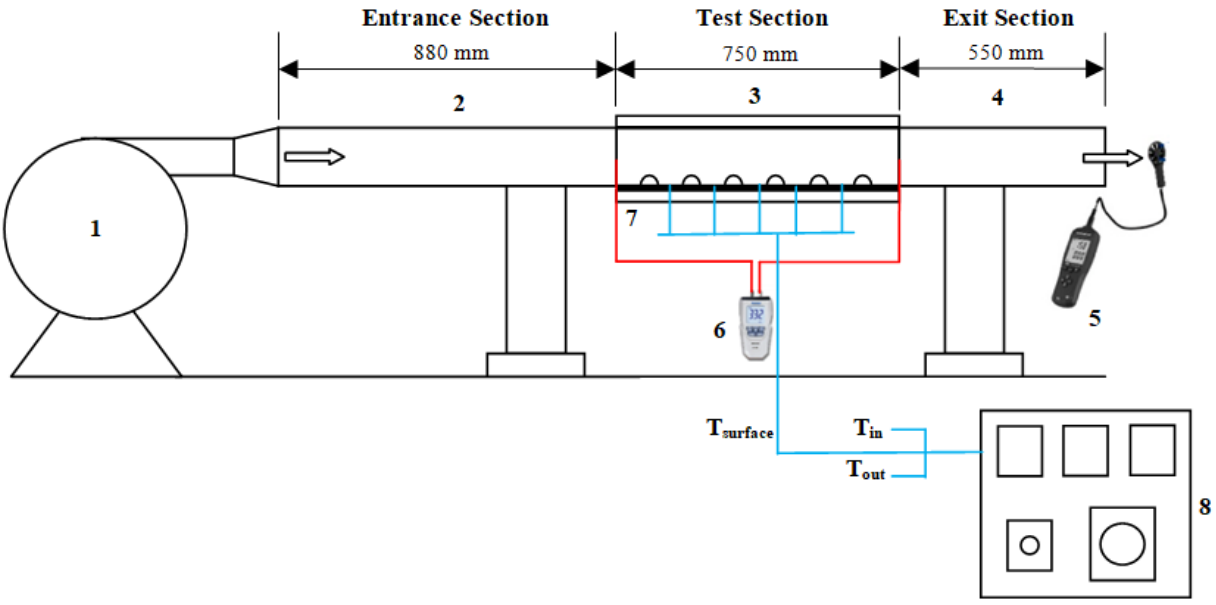

Figure 1. Diagrammatic view of the test configuration

Figure 2. Photograph view of the setup of the experiment

Through the use of a circular pipeline with a transition section at the end connecting the blower outlet to the duct, the blower draws ambient air into the rectangular duct. At the blower inlet is a manually operated valve that controls the duct's airflow. Aluminum plates with different semi-circular rib shapes are lined up along the bottom wall of the test section. An electric heater heats the bottom plate, and a variac transformer controls the heat flow. An anemometer was mounted near the duct's outflow to measure air velocity and calculate the air flow rate. The air temperatures at the test section's intake and exit were measured with thermocouples. The surface temperatures of the test plate were measured using K-type thermocouples positioned at various positions on its surface. The pressure differential across the test segment was measured with a digital micromanometer connected to the pressure taps at the section's entrance and exit. The instruments used in the experiment were calibrated correctly. After reaching a steady state, which usually took two to three hours, experimental data was recorded.

The aluminum test plate utilized had dimensions of 750 x 110 mm in length and width, and 5 mm thickness. The test section measured 750×110×110 mm (length, width, and height, respectively). Various configurations of the semi-circular ribs were attached to the test plate by a thin layer of adhesive capable of withstanding high temperatures. The heater was attached to the bottom side of the test plate and inserted into a rectangular duct. A constant heat flux was applied via a heater placed in contact with the bottom side of the test plate. Insulation made of glass wool was placed after the heater and around the entire test section to lessen heat loss through the test section channel. Figures 3 and 4, respectively, show a schematic design and a photographic representation of the semi-circular rib that is attached to the test plate.

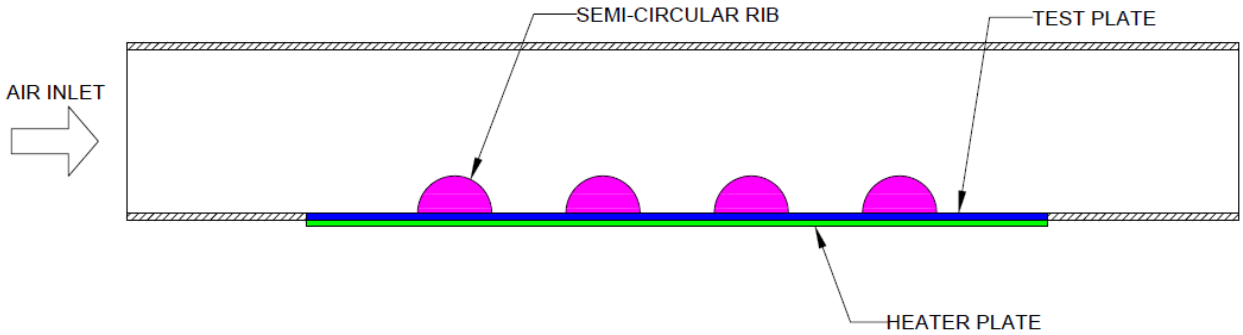

Figure 3. Schematic diagram of semi-circular rib attached to test plate in test section

Figure 4. Photographic view of semi-circular rib attached to test plate in test section

The detailed section view of the test section is shown in Figure 5.

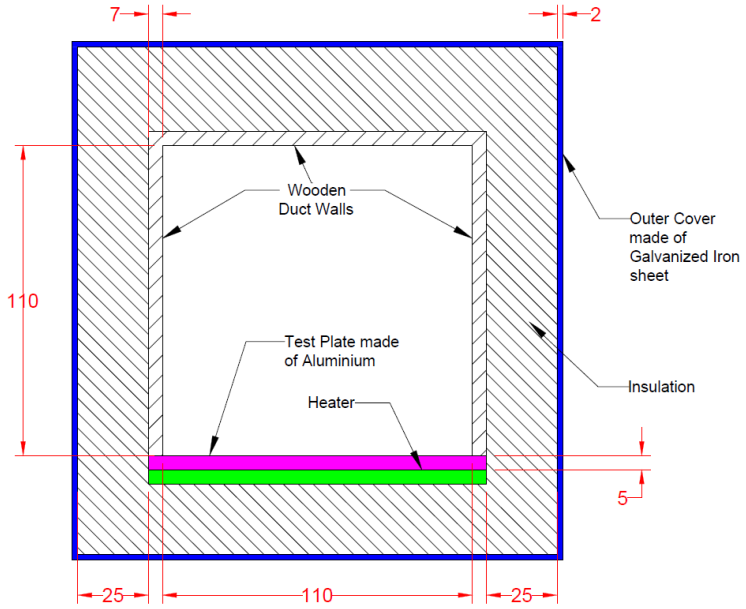

Figure 5. Detailed sectional view of test section (dimension in mm)

The top view schematic diagram of test plates with six distinct semi-circular rib configurations is shown in Figure 6.

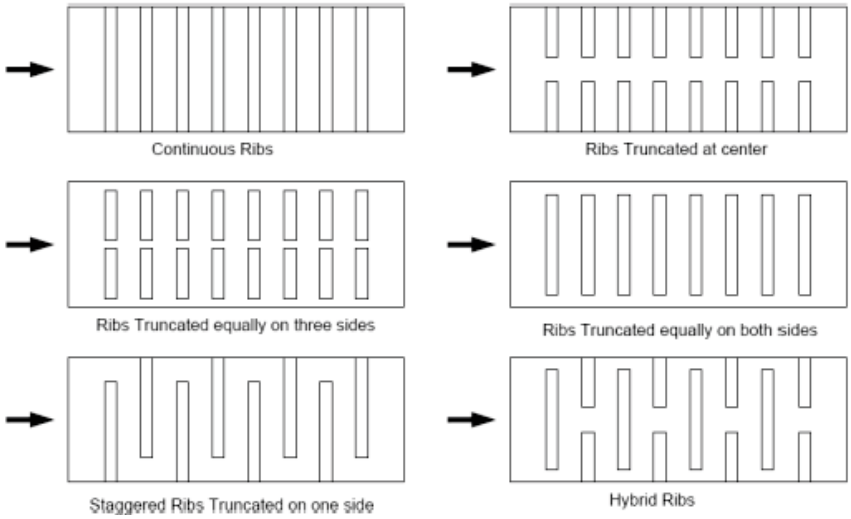

Figure 6. Schematic diagram representing the top view of Semi-circular rib configurations

Figure 7 displays photographic images of test plates that were supplied with various rib arrangements.

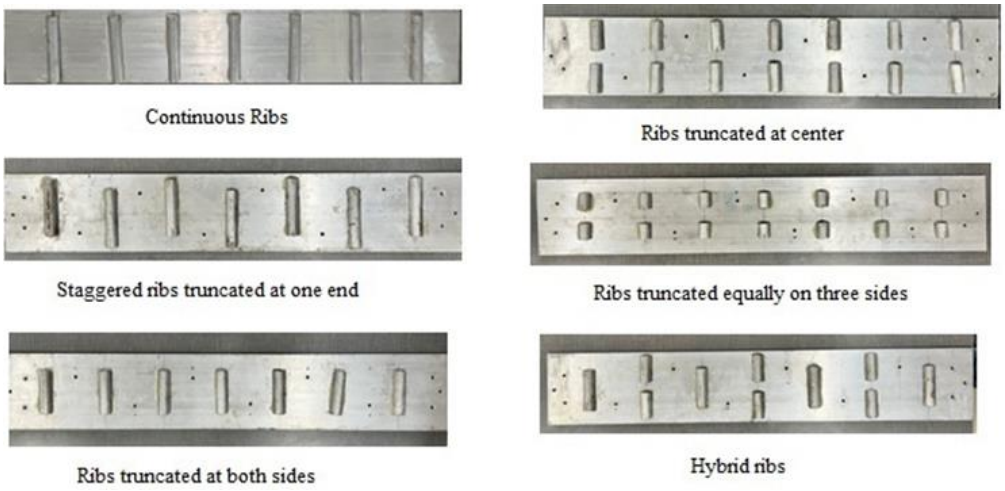

Figure 7. Photographic views of Semi-circular rib configurations

2.1 Validation of Experimental Results

This section particularizes on the validation process for experimental results obtained from tests conducted on a plain duct, utilizing various correlation data available from past research. The goal of this validation was to validate the experimental findings regarding friction factor and transfer of heat obtained for the plain duct by comparing them with established correlation data specifically applicable to plain duct configurations. In Table 1, Nusselt number values for the plain rectangular channel derived from experimental data and correlations are compiled.

Table 1. Nusselt number values for plain duct

Sr. No.	Reynolds Number	Experimental Nusselt number (Nu)	Theoretical Nusselt number by Dittus-Boelter equation	Theoretical Nusselt number by Abdel-Moneim correlation
1	13531	44.22	40.57	43.95
2	17617	56.14	50.10	54.27
3	23078	68.25	62.18	67.36
4	28535	78.38	73.69	79.83
5	34676	90.99	86.13	93.30

The Nusselt number that has been determined from experiments varied between 5.65% and 12.06% relative to theoretical outcomes. Similarly, the variation in experimental values for Nusselt numbers was discovered to be between 0.62% and -2.48% when compared to the Abdel-Moneim correlation values. The comparison reveals that the Abdel-Moneim correlation and the investigational Nusselt Number values are more similar than the Dittus-Boelter correlation [33]. In Table 2, friction factor values for the plain rectangular channel derived from experimental data and correlations are compiled.

Table 2. Friction factor values for plain duct

Sr. No.	Reynolds Number	Experimental Friction Factor (f)	Friction factor by Blasius Equation	Theoretical friction by Darcy's equation
1	13531	0.0316	0.0293	0.0290
2	17617	0.0280	0.0274	0.0270
3	23078	0.0273	0.0256	0.0252
4	28535	0.0251	0.0243	0.0239
5	34676	0.0243	0.0232	0.0228

It was discovered that, in comparison, the experimental and theoretically calculated friction factor values were quite similar. The friction factor values in theory and experiment for the plain duct were compared. The finding was made that the variation in experimental friction factor values ranged from 3.67% to 9.03% when compared to the values obtained from Darcy's equation. Similarly, the finding was made that the variation in experimental friction factor values ranged from 2.13% to 7.81% relative to the values found from the Blasius equation. This implies that the experimental friction factor data closely resemble the Blasius equation in relation to Darcy's equation.

2.2 Error Analysis

In this research study, assessing the inherent inaccuracies in experimental measurements is paramount, as no measurement process is entirely free of flaws. A key aspect of this assessment involves distinguishing between error and uncertainty. Error is defined as the specific numerical difference between the true value of a quantity and its recorded value. In contrast, uncertainty encompasses the range within which the true value is likely to lie. Unlike error, which is a fixed and often quantifiable discrepancy, uncertainty is inherently statistical and reflects the variability inherent in the measurement process. To address this variability, the study employs established statistical techniques from the literature to calculate uncertainty. These techniques generate a range that most likely includes the true value, providing an equiprobable deviation from the parameter's most likely value, thereby offering a robust framework for understanding measurement accuracy.

For a more detailed analysis of uncertainty in the parameters derived during this study, the model proposed by Kline and McClintock [34] is utilized. This model evaluates uncertainty based on the dispersion or spread of the recorded values that form the basis of the calculations. By quantifying the degree of variability observed in the measurements, the model enables a comprehensive understanding of the experimental setup's reliability and limitations. The adoption of this approach not only highlights the uncertainties in the experimental data but also helps to contextualize the findings by providing a statistical measure of confidence. Table 3 presents further details of the uncertainty analysis, offering a clearer insight into the methodologies and results derived from applying the Kline and McClintock model in this study.

Table 3. Range of uncertainty percentage for various parameters

Sr. No.	Parameters	Uncertainty range
1	Mass flow rate of air	±5.0024%
2	Convective heat transferred to air	±9.3013%
3	Convective heat transfer coefficient	±9.3054%
4	Reynolds Number	±5.0387%
5	Nusselt number	±9.3057%
6	Experimental Friction Factor	±10.1995%

3. RESULTS AND DISCUSSIONS

Investigational data was gathered to study various aspects of the transfer of heat and the flow of fluid. The findings of these features were plotted versus Reynolds number (Re), and they are discussed in this section. To commence the research investigation, heat transfer coefficient statistics for all configurations under examination were presented and discussed. The configurations had Reynolds numbers between 13,500 and 35,000. The friction properties and Nusselt number values of several semi-circular rib turbulator shapes were subsequently compared with those of smooth or plain ducts under the same test conditions.

3.1 Heat Transfer

Figure 8 provides an illustration of the connection of Reynolds number (Re) and coefficient of heat transfer (h) when P/e ratio=8. Notably, the truncated rib structure demonstrated greater thermal transfer improvement than the continuous rib structure. Among the various rib configurations analyzed, the hybrid ribs design demonstrated the most favorable "h" values. Specifically, the values of “h” for the hybrid rib configuration were 1.17-1.57 times improved than that of the plain duct under the same operating conditions. Similarly, the rib shape with the ribs truncated equally on three sides had a 0.95–1.33 times higher coefficient of heat transmission than the plain duct. Also, rib configuration having ribs truncated at the center showed 0.81-1.27 times greater “h” values than that of the plain duct. The rib configuration, having staggered ribs truncated on one side, showed minimum and maximum rises in the coefficient of heat transfer value, which was of order 0.67 and 1.14 times larger than the plain duct, respectively. In comparison to the simple duct, the truncated rib designs exhibited superior heat transfer coefficient values. This is because the existence of truncated ribs caused the boundary layer to attach and reattach, as well as disturbances within the flow. Among the rib configurations tested, the continuous rib configuration exhibited the lowest rise in “h” values relative to the simple duct. This is because continuous rib configuration created lesser turbulence relative to the other cases of truncated rib configurations.

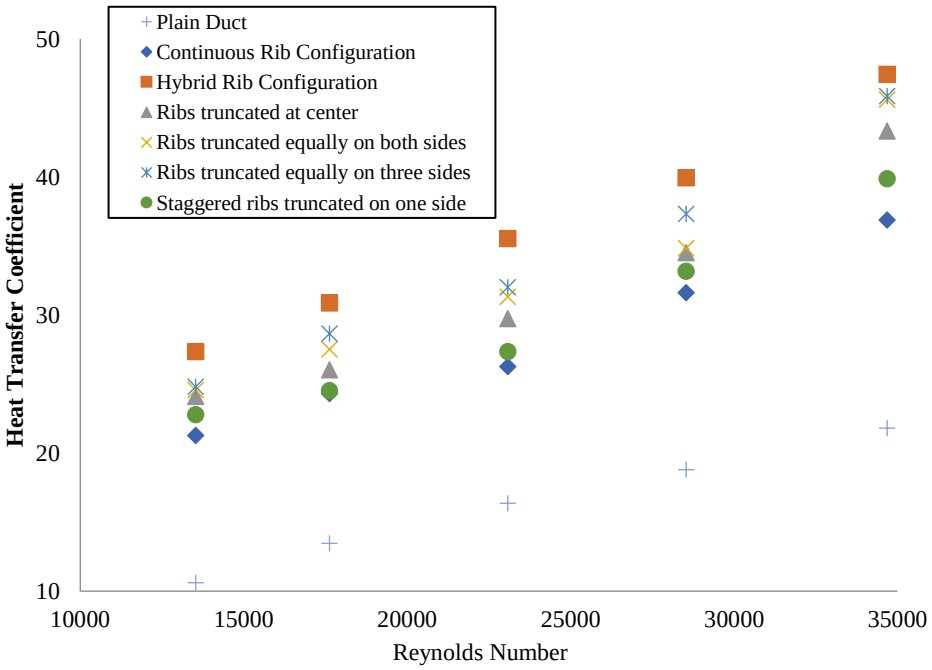

Figure 8. Figure showing convective heat transfer coefficient in relation to Reynolds number

3.2 Nusselt Number

The Nusselt number results obtained from experimental testing of a test section, both with and without various rib configurations, were analyzed to assess heat transfer variations across different rib geometrical arrangements. Figure 9

implies that increased airflow correlates with an increase in the Nusselt number. Furthermore, the rib's existence significantly improves heat transfer, with the ribbed test section consistently exhibiting higher Nusselt numbers in comparison to the simple plain duct. Additionally, observations demonstrate that the truncated semi-circular rib configurations worked better than the continuous rib configuration and plain duct. Among the rib configurations tested, continuous ribs showed the least enhancement in heat transfer but still demonstrated a notable improvement over the plain duct. However, the hybrid rib configuration outperformed all other rib configurations, resulting in a remarkable 112% to 157% increase in heat transfer for the P/e ratio = 8. This superior performance can be attributed to the geometrical arrangement of the ribs, which includes a combination of ribs truncated at the center and ribs truncated equally on both sides. Ribs having a hybrid configuration resulted in better mixing of air caused by slots provided at the center as well as at both ends of ribs. In addition, rib obstacles produced flow separation and vortices in the flow, which, in comparison to alternative arrangements, caused the air passing through the duct to receive more heat from the heated surface.

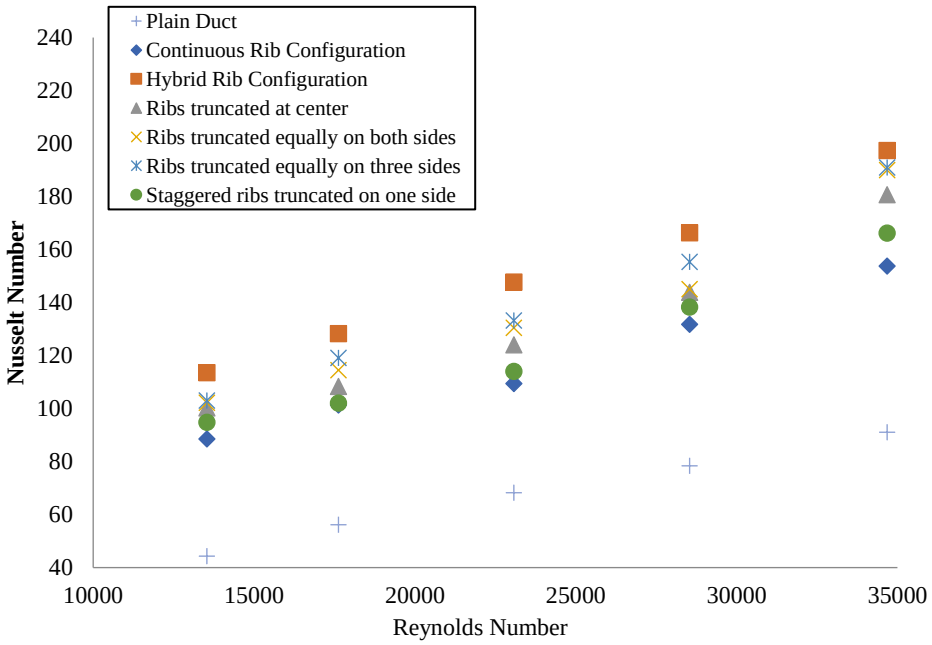

Figure 9. Nusselt number versus Reynolds number graph

With a P/e ratio =8, the minimum and maximum heat transfer rise for the rib truncated equally on three sides was 0.95 and 1.33 times that of the plain duct, respectively. In addition, the rib configuration with ribs truncated equally on both sides also exhibited a 0.85-1.31 time increase in heat transfer relative to the plain duct. Also, the rib configuration having ribs truncated at the center showed 0.82-1.27 times greater heat transfer than the plain duct. The rib structure with staggered ribs truncated on one side resulted in the transfer of heat almost 1.14 times relative to that of the plain duct. Overall, all rib designs performed significantly better in heat transfer than the plain test section.

3.3 Friction Factor

It is a critical parameter affecting the pumping power requirement in heat exchangers. Higher friction factors indicate increased resistance to flow, which translates to higher energy consumption for pumping fluids through the system. Ribbed surfaces introduce disturbances in the flow, leading to increased friction factors compared to plain ducts. The ribs act as obstacles, creating additional turbulence and thereby increasing pressure drop. The friction factor results obtained from experimental testing of a test section, both with and without various rib configurations, were analyzed to assess how each configuration influences flow resistance and, consequently, pressure drop. This comparison helped identify the effective rib geometries among tested rib geometries in reducing or enhancing pressure drop. For various P/e ratios, The friction factor's relationship to the Reynolds number is seen in Figure 10.

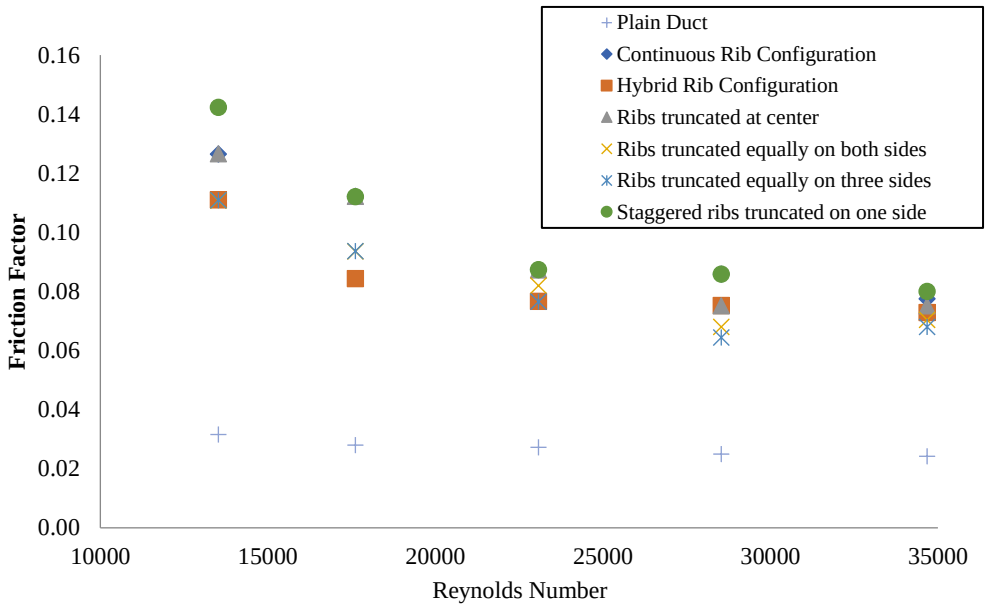

Figure 10. Friction factor vs Reynolds number graph

It is observed that rib configurations with ribs truncated at the center and ribs truncated on both sides showed comparatively lower increases in friction factor than staggered and continuous ribs. This suggests that these configurations are more conducive to reducing pressure drop while still promoting heat transfer enhancement compared to more obstructive rib designs. For configurations with ribs truncated on both sides and ribs truncated in the center, the friction factor rises by 1.72-2.51 and 2.00-3.01 times, respectively, relative to the plain duct. The hybrid rib arrangement, which combines elements of various rib designs, exhibits an intermediate increase in friction factor within the range of 1.81-2.52 times that of the simple duct. This suggests a balance between promoting turbulence and minimizing blockages, resulting in moderate pressure drop compared to both plain duct and highly obstructed rib configurations. Rib configuration having ribs truncated equally on three sides reveals the least rise in friction factor among all the tested rib configurations, and it is observed to be within 1.58-2.51 times relative to plain duct.

3.4 Overall Enhancement Ratio/ Thermal Performance

Figure 11 indicates that the duct's thermal performance declines as the Reynolds number rises. This decline is attributable to several factors. First, when Reynolds numbers grow, the time the air spends crossing the duct decreases, resulting in fewer exchanges of heat to the air. Additionally, higher air velocities at higher Reynolds numbers result in increased turbulence, which in turn lowers the Nusselt number ratio. Nevertheless, all the examined rib designs exhibit rising thermal performance at 5.1 m/s. The turbulence created at this speed results in improved heat transfer, leading to this effect. Since thermal performance is closely associated with the Nusselt number ratio, this decline in the duct's thermal performance with an increase in Reynolds numbers can be attributed to these interrelations. The superior performance of the hybrid rib configuration can be attributed to its ability to enhance flow turbulence, increase surface area for heat transfer, optimize flow distribution, reduce thermal resistance, and capitalize on the synergistic effects of combined rib designs. These factors work together to make the hybrid configuration more effective at improving thermal performance than traditional ribbed designs.

The findings derived from Figure 11 highlight a significant revelation regarding the thermal performance of various rib configurations in heat exchangers. The data indicates that the hybrid rib configuration consistently demonstrates superior thermal performance across all examined Reynolds numbers when compared to the other tested rib designs. Specifically, the enhancement in thermal performance for the hybrid rib configuration ranges from 1.47 to 1.69 times greater than that of the plain duct configuration. This substantial improvement underscores the effectiveness of hybrid ribs in optimizing heat transfer, likely due to their unique design that combines different geometries and potentially augments turbulence and mixing within the airflow. In contrast, the continuous rib configuration exhibits the least improvement in thermal performance among the investigated rib layouts, with a modest enhancement ranging from 1.09 to 1.26 times compared to the plain duct. This minimal improvement can be attributed to the continuous nature of the rib's design, which may induce a form of blockage that, while promoting some degree of turbulence, does not enhance the heat transfer efficiency to the same extent as the more variable hybrid configurations.

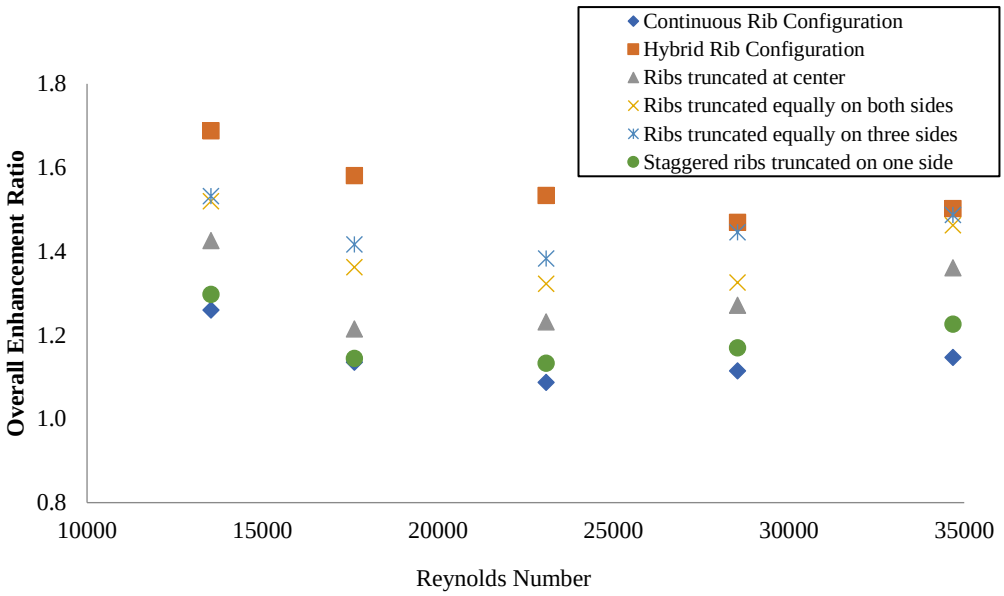

Figure 11. Thermal performance graph vs Reynolds number

Moreover, the other configurations analyzed, which include ribs that are truncated at the center, truncated equally on both sides and truncated equally on three sides, exhibit thermal performances that, while lower than the hybrid ribs, are superior to that of the continuous ribs. This finding suggests that the truncation of ribs can be an effective design strategy to balance airflow disruption and thermal enhancement. The results imply that while the hybrid rib design is optimal, other truncated configurations can still provide viable alternatives depending on specific application requirements. The analysis of these configurations highlights the importance of rib design in optimizing thermal performance in duct systems. The distinct advantages of the hybrid rib configuration emphasize the need for further exploration of mixed geometry designs, which can harness the benefits of different shapes to achieve higher heat transfer rates.

4. CONCLUSIONS

The goal of this study is to use experimental methods to investigate the impact of various geometrical arrangements of continuous and truncated semi-circular ribs on the thermal efficiency of a rectangular duct. The experimental results for a smooth duct were compared to those for ducts with semi-circular rib designs under identical flow circumstances to evaluate potential enhancements in heat transmission and friction factor. To support these conclusions, actual data on the friction factor and Nusselt number from plain ducts were compared to results from theoretical formulas that include the Dittus-Boelter correlation and the Blasius equation.

The principal findings of the current study indicate that the experiment revealed a superior thermal performance of ducts equipped with hybrid ribs, which was observed to be between 1.47 and 1.69 times higher compared to plain ducts. This hybrid rib design demonstrates significant potential for various applications where efficient heat transfer is crucial. By integrating different rib geometries, materials, or orientations, hybrid ribs considerably enhance thermal performance, improving heat transfer efficiency and diminishing thermal resistance. This advancement in hybrid rib technology bolsters thermal management across various industries, including HVAC, electronics, automotive, aerospace, and renewable energy. Such innovations pave the way for more compact, energy-efficient, and reliable thermal systems, potentially leading to reduced energy consumption, enhanced operational performance, and extended lifespans of critical components.

Furthermore, the continuous and staggered ribs showed the highest friction factors among the various configurations tested, attributed to their capacity to induce greater blockages and turbulence in airflow. Notably, the continuous rib configuration displayed a peak penalty regarding pressure loss within the analyzed Reynolds number range, with the average friction factor escalating by 320% to 451% compared to that of a plain duct. Additionally, in this experimental study, the Nusselt number ratios varied from 1.44 to 2.57, while the friction factor ratios ranged from 2.20 to 4.51. Throughout the study, it was observed that the experimental Nusselt number values deviated by 5.65% to 12.06% relative to those derived from the Dittus-Boelter equation. Similarly, the deviation in experimental Nusselt number values compared to the Abdel-Moneim correlation was found to range from 0.62% to -2.48%. The study also revealed that the Nusselt number and friction factor of the hybrid rib structure increased by a maximum of 2.57 and 4.51 times, respectively, relative to a smooth surface. Observations indicated that the experimental friction factor values varied from 2.13% to 7.81% when contrasted with the values obtained using the Blasius equation. Moreover, an uncertainty analysis was conducted using the variability found in the raw data to predict the uncertainties associated with the experimental outcomes. The uncertainty for the friction factor ranged between 4.4055% and 10.1995%, while the Nusselt number uncertainty varied from 4.6378% to 9.3057%.

5. FUTURE DIRECTION OF RESEARCH

To further enhance thermal performance in this field, future studies should explore several key aspects. Firstly, evaluating the use of alternative rib materials with higher thermal conductivity than aluminum, such as copper, mild steel, or brass, could significantly boost heat transfer rates for a given heat exchanger size. Additionally, analyzing rib cross-sections beyond semi-circular shapes, including triangular, trapezoidal, and pentagonal configurations, would provide valuable insights into their effectiveness compared to semi-circular ribs. Conducting tests at different P/e ratios is also essential to determine their impact on overall thermo-hydraulic performance, especially since the current study utilized a P/e ratio of 8. Moreover, implementing combined heat transfer enhancement techniques, such as integrating semi-circular ribs with twisted tape inserts, could reveal potential performance gains. Lastly, investigating additional semi-circular rib configurations not employed in this study would contribute to a deeper understanding of their influence on thermal performance.

ACKNOWLEDGEMENTS

The authors acknowledge the technical support extended by the Mechanical Engineering Department of Sanjay Ghodawat Institute, Atigre (India) and Maratha Mandal's Engineering College, Belgavi (India), for providing the research facilities.

Funding: This study was not supported by any grants from funding bodies in the public, private, or not-for-profit sectors.

CONFLICT OF INTEREST

The authors report there are no competing interests to declare.

AUTHORS CONTRIBUTION

Swapnil Thikane: Methodology, Experimental Investigation, Draft Preparation, Reviewing and Editing

Suresh Mashyal: Methodology, Supervision

REFERENCES

[1] S. Thikane and S. Mashyal, "A comprehensive review and comparative study of various rib configurations used in rectangular duct for heat transfer enhancement," *Asian Review of Mechanical Engineering*, vol. 11, no. 1, pp. 33-39, 2022.

[2] S. Thikane and S. Mashyal, "A comprehensive review and comparative study of various rib configurations used in rectangular duct for heat transfer enhancement," *International Journal of Management, Technology and Engineering*, vol. 13, no. 11, pp. 1-8, 2023.

[3] S. Thikane and S. Mashyal, "A comprehensive review and comparative study of various rib configurations used in rectangular duct for heat transfer enhancement," *International Journal of Innovative Research in Technology*, vol. 09, no. 05, pp. 238-245, 2022.

[4] R. Karwa, S. Solanki, and J. Saini, "Thermo-hydraulic performance of solar air heaters having integral chamfered rib roughness on absorber plates," *Energy*, vol. 26, pp. 161-176, 2001.

[5] M. Sahu and J. Bhagoria, "Augmentation of heat transfer coefficient by using 90° broken transverse ribs on absorber plate of solar air heater," *Renewable Energy*, vol. 30, pp. 2057-2073, 2005.

[6] S. Alfarawi, S. Abdel-Moneim and A. Bodalal, "Experimental investigations of heat transfer enhancement from rectangular duct roughened by hybrid ribs," *International Journal of Thermal Sciences*, vol.118, pp. 123-138, 2017.

[7] S. Kore, S. Dingare, S. Chinchanikar, P. Hujare, and A. Mache, "Experimental Analysis of different shaped ribs on heat transfer and fluid flow characteristics," *E3S Web of Conferences*, vol. 170, pp. 01-19, 2020.

[8] J. Park, J. Han, Y. Huang and S. Ou, "Heat transfer performance comparisons of five different rectangular channels with parallel angled ribs," *International Journal of Heat Mass Transfer*, vol. 35, pp. 2891-2903, 1992.

[9] J. Liu, J. Gao, T. Gao, and X. Shi, "Heat transfer characteristics in steam-cooled rectangular channels with two opposite rib-roughened walls," *Applied Thermal Engineering*, vol. 50, pp. 104-111, 2013.

[10] N. Deo, S. Chander and J. Saini, "Performance analysis of solar air heater duct roughened with multi-gap V-down ribs combined with staggered ribs," *Renewable Energy*, vol. 91, pp. 484-500, 2016.

[11] R. Karwa, "Experimental studies of augmented heat transfer and friction in asymmetrically heated rectangular ducts with ribs on the heated wall in transverse, inclined, V-continuous and V-discrete pattern," *International Communications in Heat Mass Transfer*, vol. 30, no. 2, pp. 241-250, 2003.

[12] E. Momin, J. Saini and S. Solanki, "Heat transfer and friction in solar air heater duct with V-shaped rib roughness on absorber plate," *International Journal of Heat Mass Transfer*, vol. 45, pp. 3383-3396, 2002.

[13] S. Singh, S. Chander and J. Saini, "Heat transfer and friction factor correlations of solar air heater ducts artificially roughened with discrete V-down ribs," *Energy*, vol. 36, no. 8, pp. 5053-5064, 2011.

[14] S. Singh, S. Chander and J. Saini, "Thermo-hydraulic performance due to relative roughness pitch in V-down rib with gap in solar air heater duct-comparison with similar rib roughness geometries," *Renewable and Sustainable Energy Reviews*, vol. 43, pp. 1159-1166, 2015.

[15] N. Sharma, A. Tariq and M. Mishra, "Detailed heat transfer and fluid flow investigation in a rectangular duct with truncated prismatic rib," *Experimental Thermal and Fluid Science*, vol. 96, pp. 383-396, 2018.

[16] N. Sharma, A. Tariq, and M. Sharma, "Experimental investigation of heat transfer enhancement in rectangular duct with pentagonal ribs," *Heat Transfer Engineering*, vol. 40, pp. 147-165, 2019.

[17] N. Fifi, A. Abdala, and Q. Zheng, "Effects of curved ribs on heat transfer, friction and exergy loss in rectangular cooling channels by CFD," *Iranian Journal of Science and Technology*: *Transactions of Mechanical Engineering*, vol. 45, pp. 1045-1056, 2021.

[18] H. Ali and A. Munther, "Numerical investigation on heat transfer enhancement and turbulent flow characteristics in a high aspect ratio rectangular duct roughened by intersecting ribs with inclined ribs," *Journal of Engineering*, vol. 26, pp. 20-37, 2020.

[19] S. Zahran, A. Sultan, M. Bekheit and M. Elmarghany, "Heat transfer augmentation through rectangular cross section duct with one corrugated surface: An experimental and numerical study," *Case Studies in Thermal Engineering*, vol. 36, pp. 1-14, 2022.

[20] S. Thikane and S. Mashyal, "Experimental investigation of effect of different configurations of semi-circular or half-round ribs on heat transfer enhancement in a rectangular duct," *Mechanics Based Design of Structures and Machines*, vol. 52, no. 12, pp. 10646-10662, 2024.

[21] S. Thikane and S. Mashyal, "Experimental investigation of effect of different configurations of semicircular or half round ribs on heat transfer enhancement in a rectangular duct," *2023 IEEE Engineering Informatics*, Melbourne, Australia, pp. 1-6, 2023.

[22] A. S. Yadav and A. Gattani, "Revisiting the influence of artificial roughness shapes on heat transfer enhancement," *Materials Today: Proceedings*, vol. 62, pp. 1383-1391, 2022.

[23] A. S. Yadav and A. Gattani, "Solar thermal air heater for sustainable development," *Materials Today: Proceedings*, vol. 62, pp. 80-86, 2022

[24] A. S. Yadav, A. Agrawal, A. Sharma, and A. Gupta, "Revisiting the effect of ribs on performance of solar air heater using CFD approach," *Materials Today: Proceedings*, vol. 63, pp. 240-252, 2022.

[25] A. S. Yadav, A. Agrawal, A. Sharma, S. Sharma, R. Maithani, and A. Kumar, "Augmented artificially roughened solar air heaters," *Materials Today: Proceedings*, vol. 63, pp. 226-239, 2022.

[26] A. S. Yadav, A. Mishra, K. Dwivedi, A. Agrawal, A. Galphat, and N. Sharma, "Investigation on performance enhancement due to rib roughened solar air heater," *Materials Today: Proceedings*, vol. 63, pp. 726-730, 2022.

[27] A. S. Yadav and A. Sharma, "Experimental investigation on heat transfer enhancement of artificially roughened solar air heater," *Heat Transfer Engineering*, vol. 44, pp. 624-637, 2022.

[28] H. Singh, T. Alam, M. Haque Siddiqui, M. Ashraf Ali, and D. Sagar, "Experimental Investigation of Heat Transfer Augmentation Due to Obstacles Mounted in Solar Air Heater Duct," *Experimental Heat Transfer*, vol. 37, pp. 162-181, 2022.

[29] A. Kumar and A. Layek, "Nusselt number and friction factor correlation of solar air heater having winglet type vortex generator over absorber plate," *Solar Energy*, vol. 205, pp. 334-348, 2020.

[30] S. Zahran, A. Sultan, M. Bekheit, and M. Elmarghany, "Heat transfer augmentation through rectangular cross section duct with one corrugated surface: an experimental and numerical study," *Case Studies in Thermal Engineering*, vol. 36, pp. 1-14, 2022.

[31] A. S. Yadav, O. Shukla, A. Sharma, and I. A. Khan, "CFD analysis of heat transfer performance of ribbed solar air heater," *Materials Today: Proceedings*, vol. 62, pp. 1413-1419, 2022.

[32] A. S. Yadav, T. Alam, G. Gupta, R. Saxena, N. Gupta, K. Allamraju, et al., "A numerical investigation of an artificially roughened solar air heater," *Energies*, vol. 15, pp. 1-27, 2022.

[33] S. Abdel-Moneim, E. Atwan and A. El-Shamy, "Heat transfer and flow friction in a rectangular duct with repeated multiple V-ribs mounted on the bottom wall," *Mansora, Egypt. In: Proceedings of the 12th Int. Mechanical Power Engineering Conference (IMPEC12)*, vol. 2, pp. 11-25, 2001.

[34] S. Kline, and A. McClintock, "Describing uncertainties in single sample experiments," *Mechanical Engineering*, vol. 75, pp. 3-8, 1953.

LIST OF ABBREVIATIONS

P/e	Ratio of Pitch of rib to height of rib	m	Air flow rate, kg/s
P	Pitch, m	A	Cross sectional area of test section, m^2
e	Height of Rib, m	A_s	Surface Area of Test Section, m^2
W	Duct Width, m	h	Convective heat transfer coefficient, $W/m^2.°K$
H	Duct Height, m	Re	Reynolds number
D_h	Duct Hydraulic diameter, m	Nu	Nusselt number without inserts or ribs
η	Overall Enhancement Ratio	m	Air flow rate, kg/s
V	Velocity of air, m/s	A	Cross sectional area of test section, m^2